The sensitivity of changing the optical and thermal physical parameters of the Parabolic Trough Collector

Khaled Mohamad

Engineering department, International Ala-Too University, Bishkek, Kyrgyzstan.

This work is mainly focused on studying the sensitivity of changing the optical and thermal physical parameters of the Parabolic Trough Collector receiver unit and their corresponding impact on the thermal and optical performances, such as the thermal distribution of the heat transfer fluid along the length, the thermal distribution of both the absorber pipe and the outer cover of the receiver along the circumference and related efficiencies. In this paper, a novel experimental results of a receiver unit operating with an IR reflective mirror material inside the receiver is introduced. Besides, novel aspects of the background theory for the reviver unit related to IR reflectivity in the receiver annulus are discussed and implemented in a simulation code. A comparison between a developed model and simulation results are conducted.

Keywords: Parabolic trough collector; Heat transfer fluid; Receiver unit; Outer cover; Absorber pipe.

1. Introduction

The primary energy resources can be categorized into three classes: fossil fuel, nuclear energy, and renewable energy. The main problems with fossil fuels are the global shortage of supply and environmental problems. The burning of fossil fuels, for both power generation and the transport sector, contribute to at least 90% of global CO2 emissions [1][2]. The energy production related to CO2 emission will double by the year 2050 due to an increase in the demand for petroleum and natural gas [2]. Moreover, nuclear power generation in the energy mix is decreasing due to catastrophic events such as the Fukushima nuclear power plant in 2011. The disturbance in some part of North Africa and the Middle East have forced some countries to rethink and change their policies and refrain from building these nuclear power plants [2][3]. For these reasons, need for renewable energy resources has increased. According to the International Energy Agency, 50% of the new power infrastructure will be based on clean, sustainable energies by 2035[2]. Making it the world's largest source of power generation [2]. It could deliver about 30 % of the electricity needs by the year 2035[2][4].

Among the renewable energy resources, the concentrated solar power technologies are the most widely and mature technology. It has been utilized in 23 countries around the world at the time of writing [5]. This technology is capable of satisfying the demand for thermal energy, as well as electrical energy [4][6]. In the concentrated solar power technologies, the Parabolic Trough Collector (PTC) technology is the earliest and most widely accepted design for harnessing solar energy for the dispatchable source (it refers to the source of energy that can be used on-demand or at the request of power grid operators) of electricity or industrial and chemical, due to its low cost and reliability [7]. In this technology, solar radiation is focused onto a focal line aimed at the receiver unit, see Figure 1. The receiver heats up and in turn, imparts a significant portion of its heat to a Heat Transfer Fluid (HTF) circulating within. The hot HTF can be used to generate electricity through a steam cycle or in thermochemical applications. The receiver unit is one of the most complex parts of the PTC. Its optical and thermal properties directly influence the performance of the entire system, and the efficiency of the whole system largely depends on it [8]. Therefore, the receiver unit has to be carefully designed in such a way to minimize energy losses.

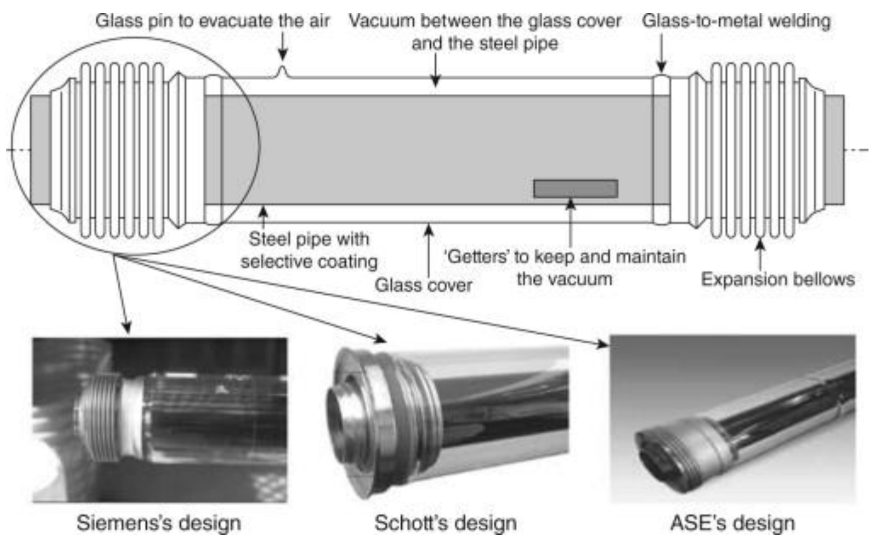

Figure 1: Parabolic Trough Collector receiver unit [9].

In Figure 1, the conventional type of the PTC receiver unit for PTC is evacuated glass metal. It consists of a blackened absorber pipe encapsulated by the glass cover. An evacuated region in between minimizes convective heat losses. The conventional receiver has advantages such as high efficiency and small heat loss. However, it has some deficiencies, such as: a) the breakage of the glass and the metal glass seal, which leads to loss the vacuum in the annular region between the metal pipe and the glass cover [10], b) lower efficiency at high temperatures [11][12], c) the permeation of hydrogen gas into the annular region due to the thermal decomposition of the organic HTF such as Therminol VP-1 [13], d) non uniform thermal distribution and thermal stress problems [12][14], e) high capital outlay and high maintenance cost [15][16].

Some complications start to appear at a high temperature (> 300 °C) and with a non-uniform solar flux distribution such as the thermal performance and thermal stress of the receiver unit. When a non-uniform heat flux profile is incident on the receiver unit, the temperature across the circumference varies, and peaks/hot spots in the receiver start to increase with temperature. It leads to bending of the absorber pipe and breaking of the glass cover. P Wang et al. [14] found that the maximum temperature gradient for the safe operation of receiver tubes is about 50 K. These complications have been addressed to increase the life span of the receive absorber. Some recent research focused on improving both thermal transfer and uniformity of the thermal distribution [12], but sacrifice pressure drop of the receiver unit or increase the quality of the absorber pipe and other components, adding cost [11].

Increasing the outlet HTF temperature is one of the main challenges to improve the overall efficiency of the PTC power plant and to reduce the Levelized Cost of energy and the combined thermal storage. For example, thermal storage quantity can be reduced to one third, if the HTF temperature increases from 350 °C to 600 °C [13]. The dominant heat losses mechanism at high temperatures is the thermal emission (IR) from the receiver pipe. This loss is conventionally minimized by painting the receiver pipe with a spectrally selective coating, which absorbs well in the visible region of the solar spectrum and emits poorly in the IR region. Much work has been published on selective coatings and improving their properties [17]. Dudley et al. [18] investigated the performance of black chrome and cermet selective coatings, and found that the Cermet had lower emissivity values and thus reduced thermal losses and improved efficiency. Forristal [19] compared six different selective coating materials to evaluate receiver unit performance. He showed that the receiver performance is susceptible to the optical properties of the selective coatings, and improving the coatings could result in significant efficiency gain. Cheryl et al.[20]. Investigated spectrally selective coating materials for CSP applications, and concluded that the ideal selective coating material should be easy to manufacture, low-cost, chemically and thermally stable in air at operating temperature of 500 °C. Because the selective coatings are placed on absorber pipe of the receiver, the receiver operation temperature is limited and hence thermal efficiency. Kennedy et al. [21] were able to successfully model a solar-selective coating composed of materials stable to 500 °C using computer-aided design software. Archimede Solar Energy (ASE) [22] manufactured the world's most advanced solar receiver tube with selective coating. It operates at temperature up to 580 °C with molten salts as HTF.

In analyzing the heat losses of the PTC receiver, all the heat exchange from the absorber and transferred by IR radiation and convection (in case of no vacuum in the annulus) are conducted away through the glass cover. Therefore, the thermal losses from the receiver are directly related to the glass envelope temperature, and it does not matter what is happening inside the glass tube [46]. Accordingly, this gives an insight into the possibility of reducing the heat losses by reducing the glass cover temperature. It can be a coated material in the inside of the glass cover (alternative to the selective coating) that is transparent to the visible region of the solar spectrum and reflects well in the IR region. A coating of this type is referred to as a "hot mirror" (or "heat mirror") and was first implemented for energy-efficient windows in automobiles and buildings [23] and for applications related to concentrating photovoltaics and thermophotovoltaics [24][25]. There are two general types of hot mirror films: a semiconducting oxide with a high doping level and a very thin metal film sandwiched between two dielectric layers (see [26][27][23] for more details). The coating with a thin metal film shows some unavoidable losses. Besides, the semiconducting oxide with a high doping level shows more advantages, i.e., Indium-Tin-Oxide (ITO). The hot mirror coating for a solar collector must meet some performance specifications. It needs to be highly transparent in the visible region and have high reflectivity in the IR region of the solar spectrum. Granqvist et al. [22] and Lampert et al. [20] investigated ways to improve the hot mirror transparency in the visible region and the reflectivity in the IR.

For PTCs, the effects of the hot mirror film have been modeled and studied previously, see Figure 2. Grena [27] simulated the system, including heat reflection using hot mirror films with simplifying assumptions, and his results showed an increase in overall efficiency over a year by 4%. Also, a 2D simulation in this regard showed the possibility of increasing the working fluid's temperature to over 400 °C [29]. Other efforts of this type used a three-dimension model to take into account the radiation exchange by different segmented surfaces inside the receiver along the pipe's length. This study showed that the hot mirror receiver effectively reduced the IR losses at higher temperatures, reduced the thermal stress on the glass cover, and suggested use in a hybrid system [30][31]. Theoretically, it was seen that hot mirror coatings will not improve on the overall efficiency of solar plants, but have the capacity of reaching much higher temperatures than their selective coating counterpart. Hot mirror type systems are currently investigated, which may, in the near future, surpass selective coating technology [31]. Further, the hot mirror coating is utilized on a cavity receiver, which is applied to the cavity opening. It showed an improvement in the optical and thermal performances of the receiver unit [32][33][11].

In this paper, the adaptations which needed to be implemented in our previously derived theory to make it useful to the experiments are discussed and constitutes a useful guide to experimenters to align their theoretical expectation with experiments. Moreover, the theoretical IR reflections model that is going to be an essential part is discussed and implemented alongside with the simulation code. These theoretical aspects and their descriptions are summarized from a more detailed account [23] in the second section.

In the third section, completely novel results related to applying an IR reflected mirror coating to the outer cover of the receiver unit of PTC, since, to our knowledge, no experiment has been performed testing the effects of this type of coating philosophy. These new results are remarkably close to our derived theoretical expectations, with the experimental results diverging from the simulation by at most 6% at around 700K, and Chi-squared test p-values around 0.99, with the worst at 0.80. The simulations underestimate the performance, indicating that better performance was measured experimentally.

The fourth section is based on the simulation results. It is a very detailed study of the solar and IR radiations interactions with the receiver unit material components. It shows how different values of the optical and thermal properties of the receiver unit components affect the efficiency of the PTC, heat transfer temperature and surface temperatures of the absorber pipe and outer cover circumferences. This study allows to investigate the expected values of optical and thermal properties required for the best candidates' materials or coating materials, as well as the right position of the coating on the receiver unit (absorber pipe or outer cover) that can provide the highest optical and thermal efficiencies.

2. Theory

A mathematical model was developed that designates the different heat transfer modes interactions inside the receiver unit, allowing for IR reflecting inside the receiver annulus, i.e., a hot mirror coating on the inside of the outer cover. This model is briefly described in this section. More detail can be found in [11][34][31]. The model uses energy conservation for the thermal interactions in the receiver, as shown in Figure 2.

.

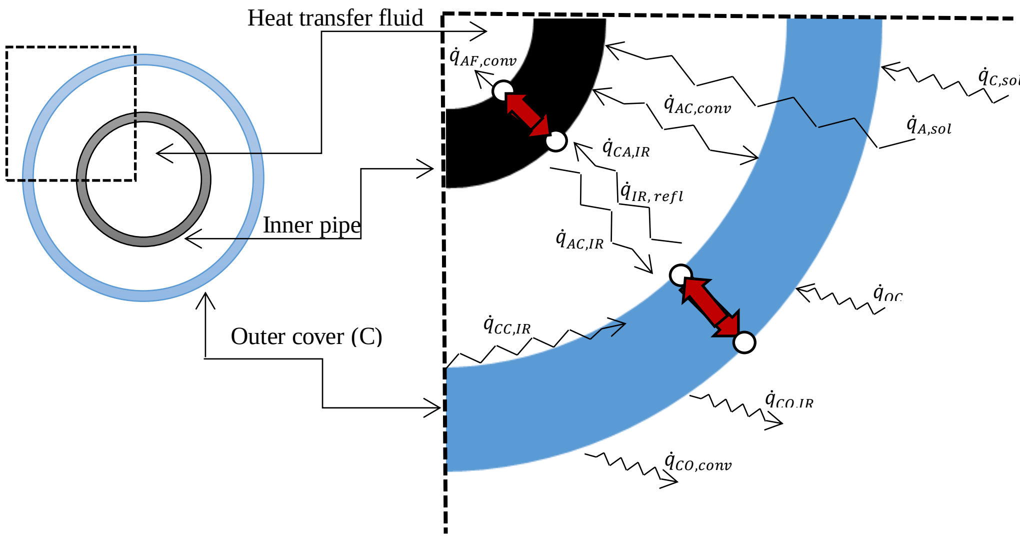

Figure 2: Heat exchanges between the outer cover, absorber pipe, heat transfer fluid, and the outside environment [31].

The concentrated solar radiation is absorbed by the Outer Cover (C), $\dot{q}_{C,sol}$ and the Absorber Pipe (AP), $\dot{q}_{A,sol}$, resulting in their temperature rise. The surfaces emit in the IR ($\dot{q}_{AC,IR}$, $\dot{q}_{CC,IR}$, $\dot{q}_{CA,IR}$) which is either absorbed, transmitted or reflected $\dot{q}_{IR,refl}$ by the intercepting surfaces, or else lost to the outside ($\dot{q}_{CO,IR}$). Notably, the existence of an IR reflecting coating on the inside outer cover results in the foremost reflection of IR in the receiver annulus. Convection heat transfer is an essential mode of heat transfer from the absorber pipe to the HTF $\dot{q}_{AF,conv}$ and from the outer cover to the outside, $\dot{q}_{CO,conv}$.

In this model, a finite volume method (FVM) is used to discretize the absorber pipe, outer cover, and the Heat Transfer Fluid (HTF) into Control Volumes (CV) along the circumference and the axial direction. The conservation of energy is applied for each CV and has the form

$$\left(\sum \dot{q}_{cond} + \sum \dot{q}_{rad} + \sum \dot{q}_{conv} + \sum \dot{q}_{sol}\right)_j = 0 \tag{1}$$

The absorber pipe and the outer cover are under steady-state conditions, where the net heat flux due to conduction $\dot{q}_{con}$, radiation $\dot{q}_{rad}$, convection $\dot{q}_{conv}$, and solar radiation $\dot{q}_{sol}$ are defined. The heat absorbed by the HTF along a single control volume is given by the equation

$$\left(\dot{q}_{AF,conv}\right)_j = \dot{m}C_p\left(T^F_{j+1} - T^F_j\right) \tag{2}$$

The Fourier law was applied to compute the conduction heat transfer, while Newton's law of cooling was used in conjunction with the Gnielinski correlation [35] to compute the convective heat transfer. Radiation heat transfer (in visible and IR) was defined as originating from every single CV onto the view of other CV resulting in surface property dependent interaction. Up to two consecutive reflections are considered.

The detailed numerical model with the derivation of the IR reflection mechanism inside the annulus, as well as the simulation implementation is completely described in [11][34]. In section three, the experimental setup for measurement of the receiver unit performance indoors under controlled heating conditions is discussed. The adaptation of the theoretical model for the receiver unit operating indoor and the corresponding simulation code were changed accordingly. The simulation provides numerical values for the temperature of the HTF along the length of the pipe, the temperature profile of the absorber pipe and outer cover along the circumference and details of the heat losses resulting from the various mechanisms. Therefore, the thermal efficiency of the system can be inferred, i.e., efficiency to convert incoming solar radiation into the internal energy of the HTF.

Efficiency is calculated using the ratio of heat gain in the fluid to the total incident solar energy, which takes all the possible losses into account [36]. The “local” efficiency for any CV section is

$$\eta_{CV} = \frac{\left(\dot{q}_{AF,conv}\right)_j}{\left(q_{sol}\right)_j} \tag{3}$$

where q_{sol} the incident solar flux, and $\left(\dot{q}_{AF,conv}\right)_j$ is defined by equation (2). The “integrated” receiver efficiency for some number n of CV’s along the system’s length is

$$\eta = \frac{\sum_{j=1}^{n}\left(\dot{q}_{AF,conv}\right)_j}{\sum_{j=1}^{n}\left(q_{sol}\right)_j} \tag{4}$$

Practically, in many applications the conversion to electricity is desired. The total "overall" efficiency η_{total} of the solar plant and conversion to turbine work for electricity generation can be obtained using a theoretical Carnot cycle. It is for simplicity and comparative purposes and is as below:

$$\eta_{max} = \frac{\sum_{j=1}^{n}\left(\dot{q}_{AF,conv}\right)_j}{\sum_{j=1}^{n}\left(q_{sol}\right)_j} \times \left(1 - \frac{T_{res}}{T_{HTF}}\right), \tag{5}$$

with T_{res} as ambient used as the cold reservoir and T_{HTF} as HTF temperatures respectively.

3. Experiment results and code validation

A receiver unit was constructed in order to validate the theory and simulation described in the previous section. The unit was constructed as it would be used in a functional PTC but was heated by heating elements situated inside the absorber tube, as opposed to from the outside by concentrated sunlight. This required us to change the simulation code slightly in order to determine the thermal properties of the unit, and this is discussed in [30].

3.1. Experimental Results

Two experiments were implemented as outlined above. The first experiment used the above system and contained no coating on either the glass cover or the absorber pipe, and is labeled the name "Bare." This system was examined because it is the simplest scenario, so any applied coating should behave better in order to be considered. It provided an additional check on our simulation and allowed us to make fine adjustments to the experimental procedure.

The second experiment used a “hot mirror” coating on the glass cover. In the first attempt, a plastic-based, transparent material coated with ITO was used, similar to the material utilized as a hot mirror for house windows for interior climate control management. It was not rated for the temperatures experienced inside the receiver unit, hence deformed and partially melted. Subsequently, a thin, aluminum-based metal sheet with an IR reflectivity of approximately 0.92 was used (obtained from the MIRO SUN Alanod Solar Company datasheet). The sheet is not transparent to solar radiation. However, this was immaterial, since, in the experiment, the effects of IR reflectivity were tested, not of solar transparency (which was, in any case, absent in our simulation). The sheet served to mimic the effects of IR reflections inside the annulus of the receiver. The main point of the experiment was to validate the theory and the simulation, with particular emphasis on the IR reflection component, and this must hold for any values. The full description of this experiment was discussed in [37].

The results of the two experiments cases are displayed in Figure 3 and Figure 4. The power density is displayed on the horizontal axis, in units of Watts per meter, and the measured and simulated temperatures are displayed on the vertical axis, in units of degrees Celsius. Both the experimental results (EXP) and the results from the simulation (SIM) are displayed. For the receiver unit without any coating, designated “bare”, Chi-squared goodness of fit gives p-values of >0.99 for the glass cover and > 0.995 for the absorber pipe.

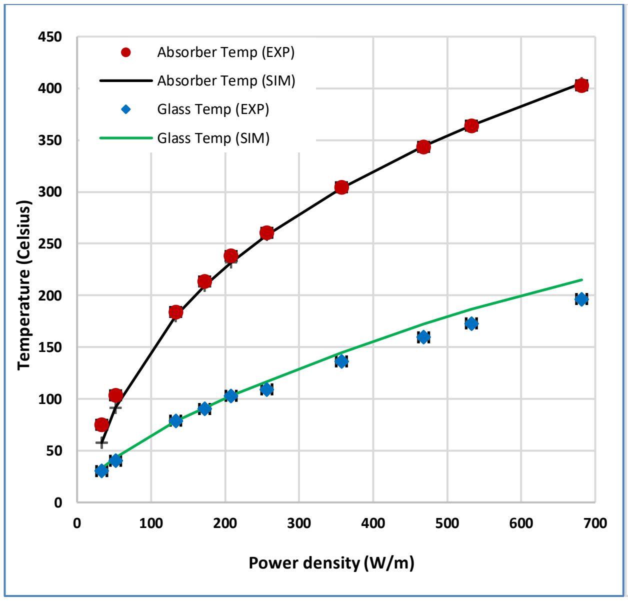

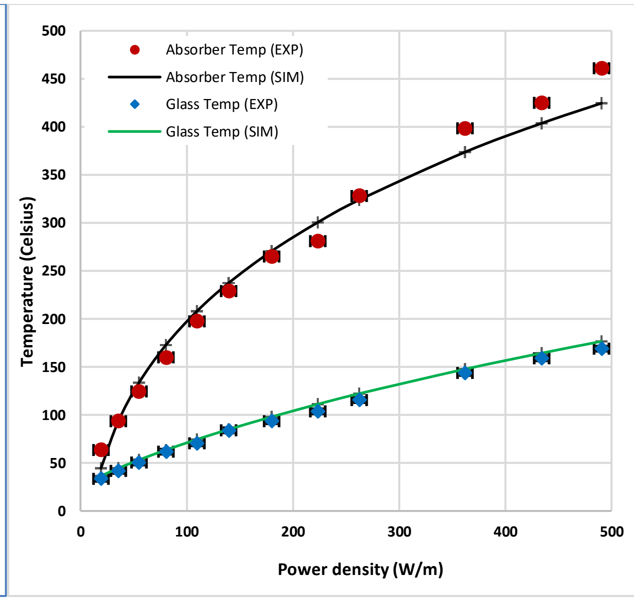

Figure 3: Experimental and simulated results for the temperature profile at different heating powers for a receiver unit without any coating, designated "bare."

Figure 4: Simulated and experimental results of the receiver unit coated with an IR reflective mirror at various temperatures.

In the second case of the receiver unit coated with an IR reflective mirror, see Figure 4. It is found that the experimental (EXP) and simulated (SIM) results for the glass cover diverge at most by 3%, while those of the absorber pipe by at most 6% at around 500 C^{o}, where the simulation underestimates the temperature. In this case, Chi-squared test gives p-values of > 0.995 for the glass cover. For the absorber pipe, a p-value of > 0.80 was obtained, and the point at 44 ^{o}C was considered an outlier, so only 10 degrees of freedom were included.

The main contribution for the divergence comes from high-temperature points, but the simulation underestimates experimental performance. This divergence is likely due to temperature dependent simulation parameters and can be addressed in a more accurate model.

It is worthy to see the effect of the coating. Consequently, the experimental data from the bare pipe and the hot mirror coated pipe are visualized in Figure 5.

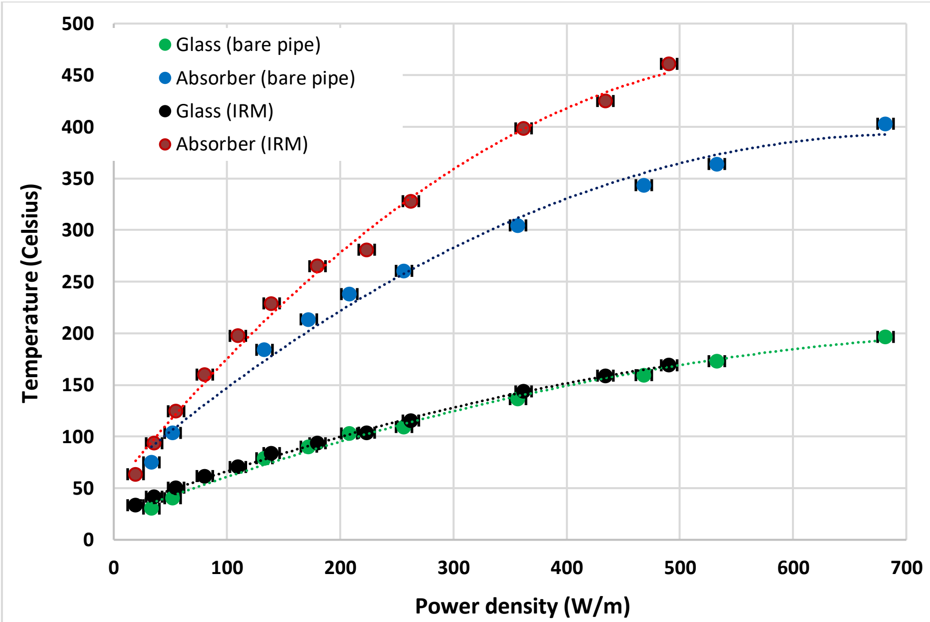

Figure 5: Comparison between experimental results from the bare pipe and IRM receiver. The hot mirror absorber pipe is capable of reaching much higher temperatures at the same power input.

The absorber pipe in the hot mirror case is considerably hotter, demonstrating better thermal retention, and would, therefore, have a better capability of heating the heat transfer fluid inside to high temperatures. The glass temperature in both cases is similar, as expected.

4. Simulation results

The validation results of our simulation shown in the previous section as well as in [34][11] allow comparison of the performance of more realistic coatings and associated efficiencies, as well as obtain thermal profiles and heat losses of the receiver unit. Our default case simulation from [31] was used in conjunction with a non-uniform solar heat flux distribution, as suggested by Jeter [38].

The simulation made use of the same operating conditions and design parameters that were used to simulate the SEGS (Solar Electric Generating System) LS2, which is one of parabolic troughs installed in the nine SEGS power plants in California [39]. The simulation parameters are shown in Table 1.

Table 1: Design parameters of the SEGS LS2 used in our simulation [28]. * stands for the bare receiver unit.

Parameter	**Parameter value**
Collector aperture	5 m
Focal distance	1.84 m
Absorber internal diameter	0.066 m

Absorber external diameter	0.07 m
Glass internal diameter	0.109 m
Glass external diameter	0.115 m
Absorber emissivity (IR)*	0.86
Absorber absorptance (visible)*	0.86
Glass emissivity (IR)	0.86
Glass transmittance (visible)	0.935
Parabola specular reflectance	0.93
Solar irradiance	933.7 W/m^2
Mass flow rate	0.68 kg/s
Wind speed	2.6 m/ s
Temperature HTF (inlet)	375.35 K
Temperature ambient	294.35 K
Incident angle	0
HTF	Molten salt

In all the calculations, we have used the optical and thermal properties for a system without any coating applications as a reference, see Table 1. The physical parameters of our interest are studied by changing their values, while the rest of the other parameters are fixed. These physical parameters are classified according to the type of electromagnetic radiation interactions with the receiver unit. First, the interaction of the receiver material components with the incident concentrated solar radiation (mostly, in the visible region of electromagnetic radiation) where a part of it is transmitted through the outer cover of the receiver. The transmitted portion of the solar radiation depends on the transmission coefficient of the outer cover (or though the aperture of the outer cover), which will be partially absorbed by the absorber pipe. The absorptivity depends on the value of the absorption coefficient of the absorber in the visible region. Second, the interaction of the receiver components with the thermal radiation in the IR region of the electromagnetic radiation. After the absorber has absorbed the solar radiation, the absorber pipe will be heated up. In this stage, the emissivity of the absorber and reflectivity/absorptivity of the outer cover in the IR region (the reflection happens inside the receiver annulus) will be a significant key for the heat loss of the receiver. Finally, investigating the effect of the thermal conductivity of the absorber material due to the non-uniform heating across the receiver circumference, which comes from the absorption of the non-uniform concentrated solar flux.

The analysis of the results is based on increment or decrement of the physical parameters that are required to be studied and comparing the corresponding simulation output results with the default simulation results (that are based on the input parameters in Table 1). The results will be in the form of percentages that represent how far the results of the corresponding particular parameter value from the results of the corresponding reference value of that parameter. Each physical parameter is going to be analyzed by answering the following questions:

- What are the percentages of changing the maximum HTF temperature values of the PTC receiver unit with specific physical parameter values and that parameter default value?
- The same question but for the maximum total efficiency.
- The same question but for the maximum difference of the temperature between the absorber pipe surface and the outer cover surface of the receiver unit at two arbitrary receiver lengths (100 m and 300 m). These lengths of the receiver unit represent the receiver unit at a relatively lower and higher temperatures.
- The same question but for the maximum temperature gradient of the absorber pipe and the outer cover circumferences.

4.1. The interaction of the receiver unit with the visible region of the incident solar radiation

The interaction of the solar radiation in the visible region of the electromagnetic radiation with the receiver is mainly related to the transmissivity of the outer cover and the absorptivity of the absorber pipe.

4.1. A. Transmissivity of the outer cover of the receiver unit in the visible region of the incident solar radiation

The transmission of the concentrated solar radiation from the parabolic trough mirror to the receiver unit through transparent material in the outer cover (C), i.e., borosilicate glass. The C transmission coefficient value limits the solar radiation transmission, so a part of the radiation is absorbed – which causes heating of the C, and another part is lost by reflection. Through this analysis, we fixed the rest of the physical parameters to study how the system performance is sensitive by changing the C transmissivity in the visible region (solar radiation). The study is carried out with an average transmission coefficient in the visible region at 0.4, 0.6, 0.8, and 0.93 (0.93 is for borosilicate glass, which is the reference value), see Table 1. The maximum HTF temperature decreased from 4% up to 21% relative to the reference, if the transmission coefficient decreased from the reference value to 0.8 and 0.4, respectively, see Figure 6. In the same order, the maximum total efficiency decreased from 18.2% up to 67.8% relative to the reference value, see Figure 7. The total efficiency is calculated using Eq. (5). Figure 8 and Figure 9 show the temperature profile of the absorber pipe and C circumference at two random lengths of the receiver 100 m and 300 m, respectively. In these figures, the angle of 180º facing the center of the collector mirror, and an angle of 0º or 360º facing the sun. Moreover, the solid and dashed lines of the same color represent the temperature profile of both absorber and C for their respective C transmission coefficient value, respectively. The maximum difference in the temperature between the absorber and C profiles significantly decreased with decreasing the transmission coefficient of the outer cover. At higher receiver temperature (at L = 300 m), this temperature difference is diminished compared to the lower receiver temperature (at L = 100 m). Furthermore, the temperature gradient across the absorber and the outer cover profiles have almost the same level of temperature reduction for higher and lower receiver temperatures, but the downtrend of the absorber temperature gradient is substantially higher than that of the outer cover, see Table 2.

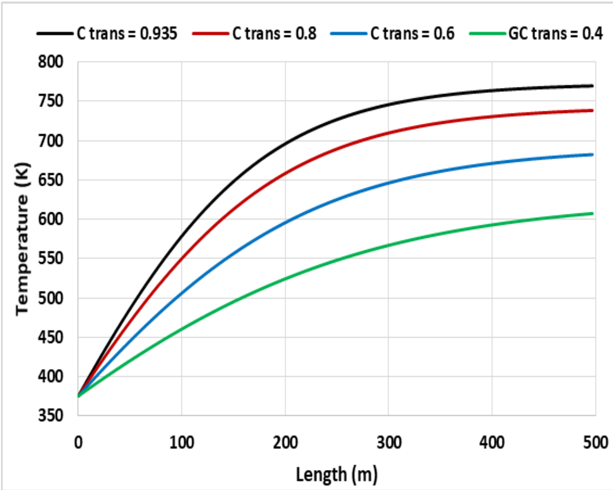

Figure 6: HTF temperature as a function of the receiver length.

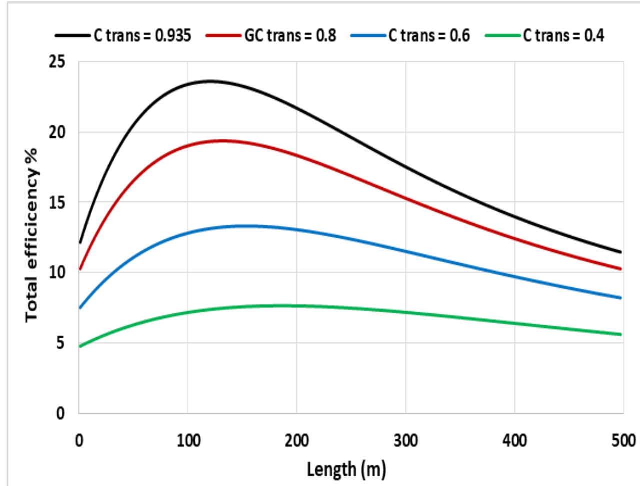

Figure 7: Total plant efficiency as a function of the receiver length.

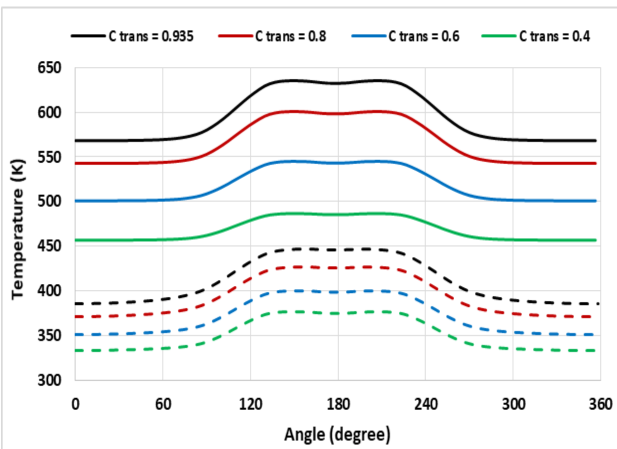

Figure 8: Absorber and outer cover temperature profiles at receiver length = 100 m.

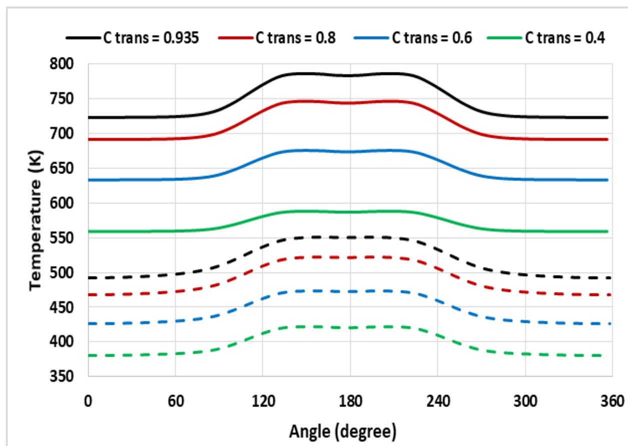

Figure 9: Absorber and outer cover temperature profiles at receiver length = 300 m.

Table 2: The changing in the outer cover transmission coefficient in the visible region. The percentages are with respect to the results of the corresponding transmission coefficient reference value (0.935). AP, C, and Δ refer to the absorber pipe, outer cover, and changing quantity, respectively.

Transmissivity	$\boldsymbol{\tau = 0.8}$	$\boldsymbol{\tau = 0.6}$	$\boldsymbol{\tau = 0.4}$
Max. HTF temp	↓ 4%	↓ 11%	↓ 21%
Max. total efficiency	↓ 18%	↓ 43.5%	↓ 68%
Max. temp. (AP – C) at 100 / 300 m	↓ 7.5% / 4.5%	↓ 22% / 14%	↓ 40% / 28.5%
Max. temp. (ΔC) at 100 / 300 m	↓ 9% / 8.5%	↓ 21.5% / 20%	↓ 31% / 30%
Max. temp. (ΔAP) at 100 / 300 m	↓ 12% / 13%	↓ 34% /33 %	↓ 55% / 53.5%

4.1. B. Absorption of the absorber pipe in the visible region of the incident solar radiation

In the visible region of the incident solar radiation, the interaction between the solar radiation and the Absorber Pipe (AP) will be only through absorption and reflection. Absorption of solar radiation by AP is the primary source of photo-thermal conversion in the Parabolic Trough Collector technology.

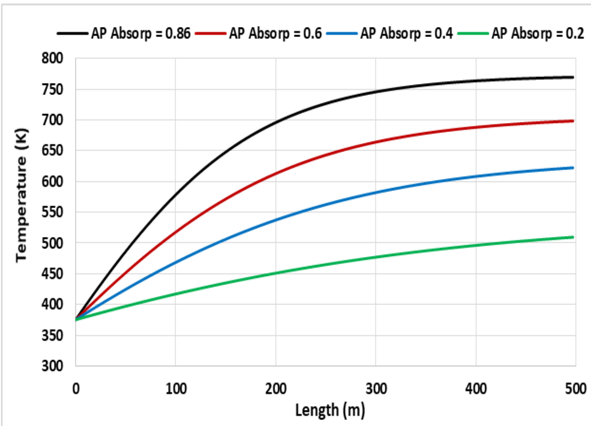

Figure 10: HTF temperature as a function of the receiver length.

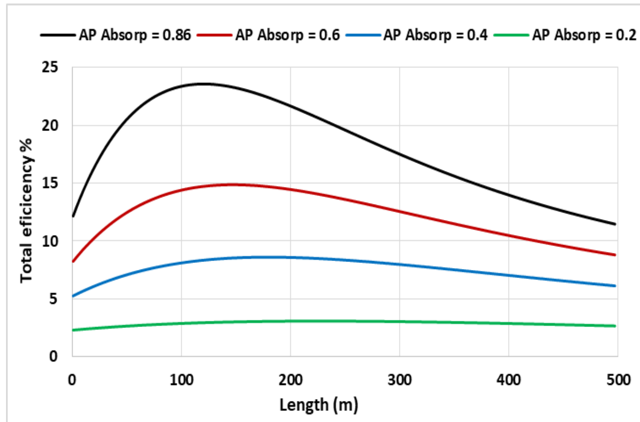

Figure 11: Total plant efficiency as a function of the receiver length.

The AP absorptivity in the visible region is studied at four different values. Heat Transfer Fluid (HTF) temperature is dramatically decreased by decreasing the AP absorption coefficient. The maximum HTF temperature decreased from 9% up to 34% relative to the reference value (Table 1) when the AP absorption coefficient decreased from the reference value to 0.6, 0.4, and 0.2, respectively, see Figure 10. In the same way, the maximum total efficiency decreased from 37% up to 87% relative to the reference, respectively, see Figure 11

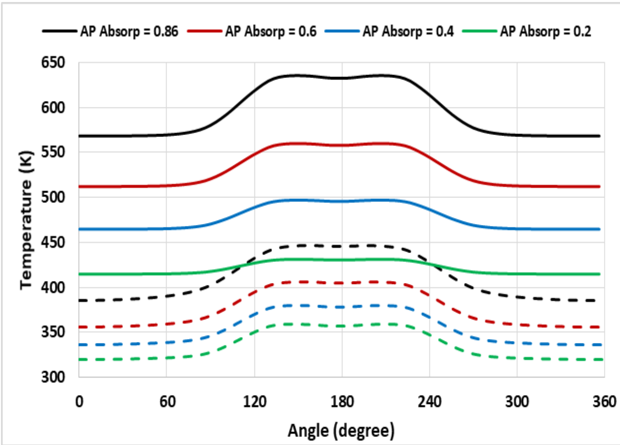

Figure 12: Absorber and outer cover temperature profiles at receiver length = 100 m.

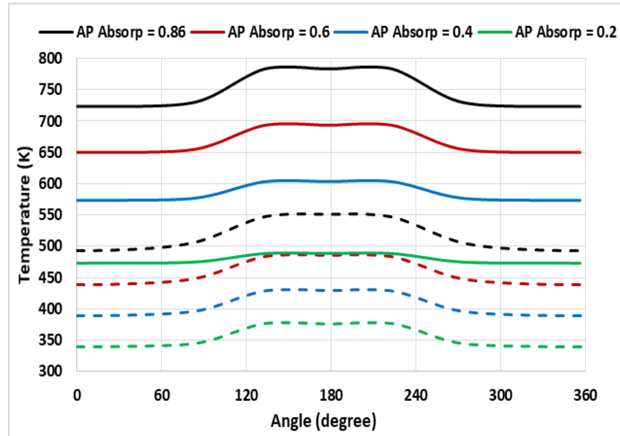

Figure 13: Absorber and outer cover temperature profiles at receiver length = 300 m.

Table 3: The changing of the absorber pipe absorption coefficient in the visible range of the electromagnetic radiation. The percentages are with respect to the results of the corresponding absorption coefficient reference value (0.86). AP, C, and Δ refer to the absorber pipe, outer cover, and changing quantity, respectively.

Absorber absorption coefficient	$\boldsymbol{\alpha = 0.6}$	$\boldsymbol{\alpha = 0.4}$	$\boldsymbol{\alpha = 0.2}$
Max. HTF temp	↓ 9%	↓ 19%	↓ 34%
Max. total efficiency	↓ 37%	↓ 63.5%	↓ 87%
Max. temp. (AP – C) at 100 / 300 m	↓ 19% / 11%	↓ 38% / 26%	↓ 62% / 53%
Max. temp. (ΔC) at 100 / 300 m	↓ 17% / 16%	↓ 28% /26.5 %	↓ 34% / 33%
Max. temp. (ΔAP) at 100 / 300 m	↓ 29% / 27.5%	↓ 52% / 50%	↓ 75.5% / 74.5%

In Figure 12 and Figure 13, the maximum temperature difference between the outer cover and AP profiles, and the maximum temperature gradient across the circumference of both outer cover and AP have the same behavior as in Figure 8 and Figure 9, but the level of temperature reduction is substantially more, see Table 3.

4.2. The interaction of the receiver unit with the IR radiation

The interaction of the thermal radiation in the IR region of the electromagnetic radiation with the receiver unit is mainly related to the reflectivity of the outer cover from the inside (IR transmissivity through the outer cover is assumed to be zero) and the emissivity of the absorber. Both are two important physical properties to control the heat losses, especially at high temperatures. Many research works have focused on a selective coating material over the absorber that has high absorptivity in the visible region and low emissivity in the IR region. Other works were focused on a material that can be coated on the outer cover from inside that has high reflectivity in the IR and high transmissivity in the visible region. In the introduction section, a literature review of some of these research works has been provided.

4.2. A. Reflectivity of the outer cover in the IR region of the electromagnetic radiation

The average reflection coefficient values of the Outer Cover (C) that were used in this analysis are 0.14 (for borosilicate glass, which is the default value), 0.4, 0.6, and 0.8. The effect of the reflectivity of C started to be effective above ~600K, see Figure 14. The maximum HTF temperature increased from 7% up to 25.3% relative to the reference, when the reflection coefficient of C increased from the reference value to 0.4 and 0.8, respectively, see Figure 14. In the same order, the maximum total efficiency increased from 8.3% up to 25.8% relative to the reference value. Generally, the effect of the C reflectivity on the temperature profiles of the receiver at L = 300 m is notably high compared to the receiver at L = 100 m length (Figure 17 and Figure 16). The receiver length of L = 300 m and 100 m represent the receiver at a relatively higher and lower temperatures, respectively. As indicated numerically by Table 4, the maximum temperature difference between C and absorber pipe is doubly increased, when the reflection coefficient increased from the reference value to 0.4, 0.6, and 0.8. The level of this temperature difference at L = 300 m is higher than the temperature difference at L = 100 m. The temperature gradient across the absorber profile does not seem to be affected by different C reflectivity for both higher and lower receiver temperatures. In the case of the temperature gradient of the C profile and with incrementing the reflectivity of C, the temperature gradient at a lower receiver temperature has a relatively lower elevation than at a higher receiver temperature case.

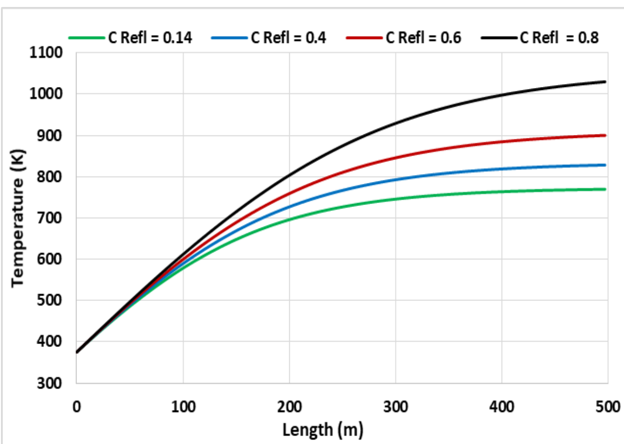

Figure 14: HTF temperature as a function of the receiver length.

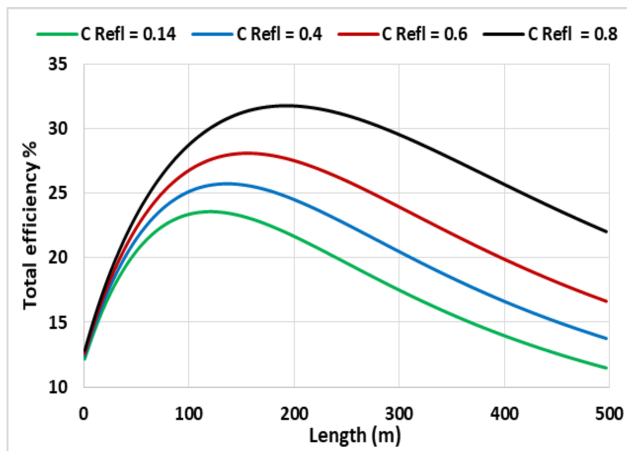

Figure 15: Total plant efficiency as a function of the receiver length.

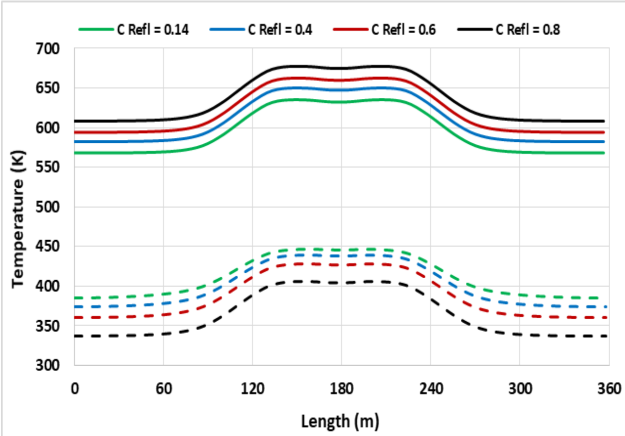

Figure 16: Absorber and outer cover temperature profiles at receiver length = 100 m.

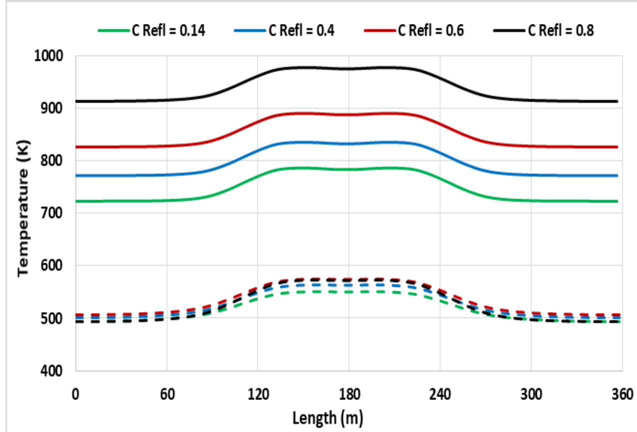

Figure 17: Absorber and outer cover temperature profiles at receiver length = 300 m.

Table 4: Changing of the outer cover reflection coefficient in the IR region of electromagnetic radiation. The percentages are with respect to the results of the corresponding reflection coefficient reference value (0.14).AP, C, and Δ refer to the absorber pipe, outer cover, and changing quantity, respectively.

Outer cover reflectivity coefficient	$\boldsymbol{\rho = 0.4}$	$\boldsymbol{\rho = 0.6}$	$\boldsymbol{\rho = 0.8}$
Max. HTF temp	↑ 7%	↑ 14.5%	↑ 25%
Max. total efficiency	↑ 8%	↑ 16%	↑ 26%
Max. temp. (AP – C) at 100 / 300 m	↑ 12% / 15%	↑ 24% / 34%	↑ 44% / 72%
Max. temp. (ΔC) at 100 / 300 m	↑ 6.5% / 7.5%	↑ 11.5% /18 %	↑ 14% / 34.5%
Max. temp. (ΔAP) at 100 / 300 m	↑ 1.2% / ~0%	↑ 2.4% / ~0%	↑ 3.4% / ~0%

4.2. B. The emissivity of the absorber pipe in the IR region of the electromagnetic radiation

The emissivity of the Absorber Pipe (AP) has a similar effect on the receiver as the effect of the reflectivity of the inside of the outer cover, where it started to be effective above ~600K. Additionally, they have the same trends for the HTF temperature and total efficiency as a function of the receiver length.

The study on the AP emission coefficient in the IR region is conducted by decreasing the average emission coefficient value from 0.86 (for bare, which is the default value) to 0.6, 0.4, and 0.2. The maximum HTF temperature is increased from 7% up to 26% relative to the default value (see, Figure 18), when the AP emission coefficient decreased from the default to 0.6, 0.4, and 0.2, respectively. Similarly, the maximum total efficiency is increased from 8.2% up to 26.5% respectively. The temperatures profiles of the outer cover and AP at receiver length L = 100 m and L = 300 m are shown in Figure 20 and Figure 22, respectively. Decreasing the value of emission coefficient tended to lower the outer cover temperature profiles and raised AP temperature profiles.

Nevertheless, with decreasing the emission coefficient value, the AP temperature profiles at a higher receiver temperature started to be notably elevated, and the outer cover temperature profiles had approximately the same temperature profiles.

The maximum temperature gradient of the outer cover profile with decrementing the AP emission coefficient is incremented with about 1.5% relative to the reference at L = 100 m and 300 m. For the temperature gradient of the AP profile, the temperature gradient at a lower receiver temperature (L=100 m) is higher than the temperature gradient of the higher receiver temperature (L=300 m), see Table 5.

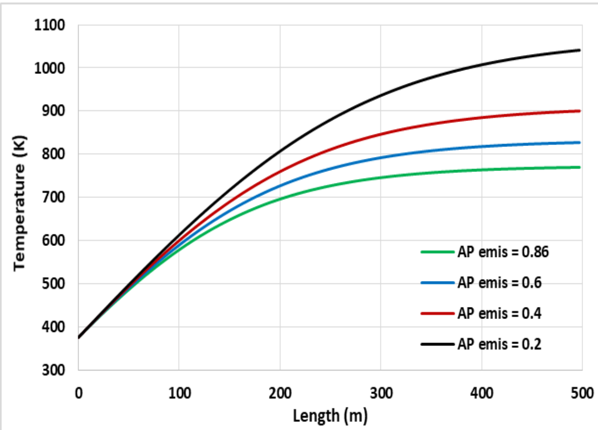

Figure 18: HTF temperature as a function of the receiver length.

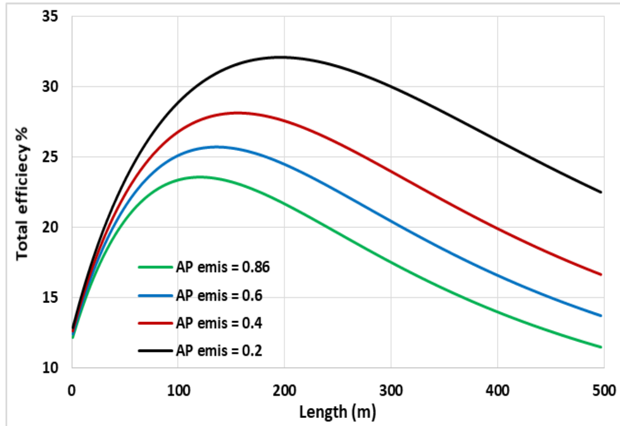

Figure 19: Total plant efficiency as a function of the receiver length.

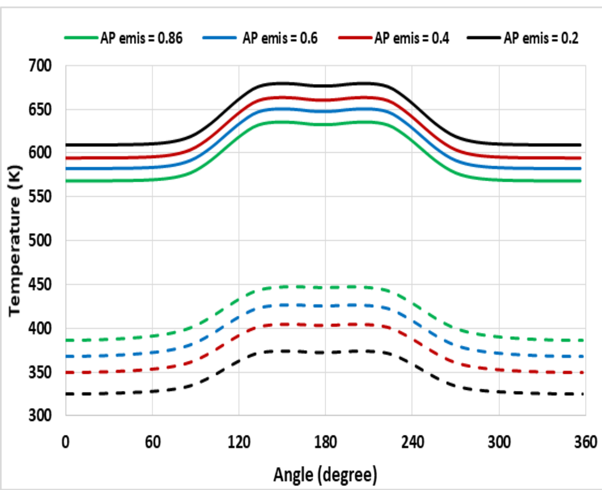

Figure 20: Absorber and outer cover temperature profiles at receiver length = 100 m.

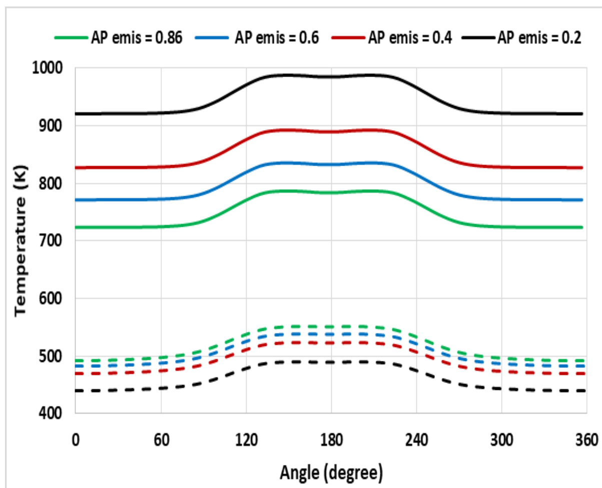

Figure 21: Absorber and outer cover temperature profiles at receiver length = 300 m.

Table 5: Changing of the absorber pipe emission coefficient in the IR range. The percentages are with respect to the results of the corresponding emission coefficient reference value (0.86).AP, C, and Δ refer to the absorber pipe, outer cover, and changing quantity, respectively.

Absorber emissivity coefficient	$\varepsilon = 0.6$	$\varepsilon = 0.4$	$\varepsilon = 0.2$
Max. HTF temp	↑ 7%	↑ 14.5%	↑ 26%
Max. total efficiency	↑ 8%	↑ 16%	↑ 26.5%
Max. temp. (AP – C) at 100 / 300 m	↑ 19% / 26%	↑ 38% / 57%	↑ 62.5% / 2 times default

Max. temp. (ΔAP) at 100 / 300 m	↓ 5% / 4.5%	↓ 11.5% /9.5 %	↓ 20% / 14.5%
Max. temp. (ΔC) at 100 / 300 m	↑ 1.5% / 1.5%	↑ 3% / 3%	↑ 4.5% / 6%

4.3. Absorber pipe thermal conductivity

Temperature gradient over the AP circumference causes many problems such as lowering the thermal efficiency, bending the AP tube, and increasing the temperature gradient over C circumference. This problem could be reduced by selecting AP material with high AP thermal conductivity. Here, the effect of the thermal conductivity of the AP has been studied at different average values, which are 16.2 (the reference value), 100, 200 and 300 W/m.K. Mainly, the AP thermal conductivity only showed an effect on the thermal distribution of the receiver unit components. As evidenced graphically and numerically by Figure 22, Figure 23 and Table 6, the maximum temperature gradient of the AP profile is decreased to 16.3%, 32%, and 42.2% relative to the reference value if the AP thermal conductivity increased from the reference value to 100, 200 and 300 W/m.K. Similarly, the maximum temperature gradient of the outer cover profile decreased to 12.4%, 23.3%, and 29% relative to the reference. Surprisingly, the temperature gradient of both AP and outer cover at L = 100 and 300 m (lower and higher receiver temperature) are precisely similar, where it is shown in Table 6 as one value for the receiver length of 100 m and 300 m.

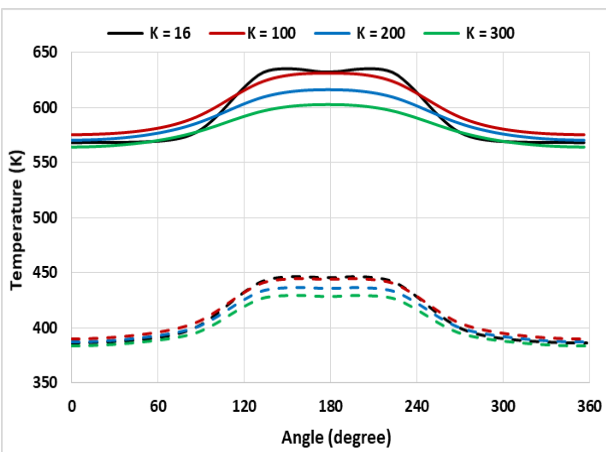

Figure 22: Absorber and outer cover temperature profiles at receiver length = 100 m.

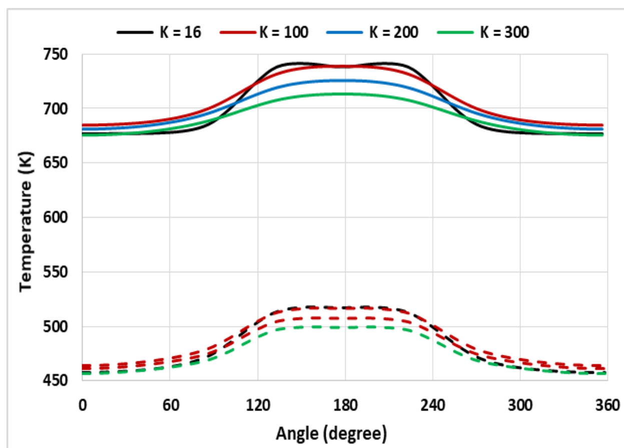

Figure 23: Absorber and outer cover temperature profiles at receiver length = 300 m.

Table 6: Changing of the absorber pipe thermal conductivity. The percentages are with respect to the results of the corresponding thermal conductivity reference value (16.2 W/m.K). AP, C, and Δ refer to the absorber pipe, outer cover, and changing quantity, respectively.

Absorber thermal conductivity	**k = 100**	**k = 200**	**k = 300**
Max. temp. (ΔAP) at 100 / 300 m	↓ 12.5%	↓ 22%	↓ 29%
Max. temp. (ΔC) at 100 / 300 m	↓ 16%	↓ 32%	↓ 42%

Reaching high values of thermal conductivity of the AP material is feasible. Metals and alloys have a variety of thermal conductivity values. For example, thermal conductivity (k) values of Steel with different doping percentages of Chrome and Nickel range are from 11.6 to 19 W/m.K at 20 ℃, while k values of Iron, Aluminum, and Copper are 69.4, 240, and 392 W/m.K, respectively at 127 ℃ [40].

5. Conclusion

The experimental results from the bare and the application of the IR mirror on the outer cover of the receiver unit indicated that the IR reflections inside the receiver were capable of higher heat retention. Further, the Chi-squared comparison between the experimental and simulated values, which yielded p-values of 0.99 for the glass cover and 0.995 for the absorber pipe on the bare pipe, and 0.995 for the glass cover and 0.80 for the absorber pipe (AP) on the IR mirror application, indicated that the model is reasonably accurate to describe an IR reflection inside the receiver unit annulus. The simulation underestimated the performance of the IR mirror at higher temperatures.

The transmissivity of the outer cover and the absorptivity of the AP in the receiver unit are the only access points of the concentrated solar radiation to enter the system for photo-thermal conversion. Heat Transfer Fluid (HTF) temperature and total efficiency are more affected by decreasing the absorptivity of the AP than the transmissivity of the outer cover. Further, the temperature difference between the AP and the outer cover, and the temperature gradient of the absorber profile are remarkably reduced by the decrement of the AP absorptivity compared to the decrement of outer cover transmissivity. However, the temperature gradient of the outer cover has an approximately similar and constant level of temperature decline while decrementing both the AP absorptivity and outer cover transmissivity.

Surprisingly, decrementing the AP emissivity and incrementing the outer cove reflectivity in the IR region have an approximately similar uptrend for the HTF temperature and total efficiency. Moreover, the outer cover reflectivity had a notable impact on distributing the heat evenly across the outer cover and the absorber profiles. However, the AP emissivity showed a better effect on increasing the temperature gap between the outer cover and the AP surface, especially at a higher receiver temperature.

The non-uniform thermal distribution across the AP circumference due to absorbing a non-uniform concentrated solar radiation caused thermal stress and reduced the longevity of both AP and outer cover of the receiver unit. It was shown that the impact of AP thermal conductivity is extensively useful for diminishing the temperature gradient across the AP and outer cover. Apart from the outer cover temperature profile is being always cooler than the absorber profile, the downtrend of the outer cover temperature gradient is remarkably lower than the temperature gradient across the absorber profile when the thermal conductivity of the absorber is incremented.

Regarding the material engineering, selecting an outer cover material that has the highest transmission coefficient in the visible region and the highest reflection coefficient in the IR region is an essential consideration for optical and thermal efficiency enhancement. Besides this, the AP material should combine the properties of having the highest absorption coefficient in the visible region and lowest emissivity in the IR region, as well as the highest thermal conductivity. We suggest that the reflectivity of the outer cover and the emissivity of the AP can be mutually used, which may depend on the receiver design. For instance, a mirrored cavity receiver can utilize the application of the IR reflective surface, i.e., hot mirror coating, on the inside of the outer cover of the receiver [41]. For the conventional receiver, It can mutually use either IR reflective surface or low emissivity surface, i.e., selective coating, over the AP of the receiver.

In the case of using the current selective coating materials, which are chemically decomposed beyond 500 C. We suggest using IR reflective coating (hot mirror) in a hybrid system. However, hot mirror type systems are currently investigated, which may, in the near future, surpass current selective coating technology [31]. If a hot mirror coating was found with better visible transmission/IR reflection properties than a selective coating, then the hot mirror would be better.

The possibility of a hybrid plant could be considered, where sections are composed of different types of coatings suitable for their temperature range.

Acknowledgments

The author would like to thank the Engineering department at Ala-Too International University for their kind support.

4. References

[1] Erdle S 2010 *The DESERTEC initiative: powering the development perspectives of southern Mediterranean countries* (Bonn: Dt. Inst. für Entwicklungspolitik)

[2] International Energy Agency (iea) *World Energy Outlook - WEO-2012* (Paris: OECD)

[3] International Energy Agency 2011 *World energy outlook 2011* (Paris: OECD)

[4] Behar O, Khellaf A and Mohammedi K 2013 A review of studies on central receiver solar thermal power plants *Renew. Sustain. Energy Rev.* **23** 12–39

[5] National Renewable Energy Laboratory (NREL) Concentrating Solar Power Projects by Country | Concentrating Solar Power | NREL

[6] Cheng Z D, He Y L and Cui F Q 2013 A new modelling method and unified code with MCRT for concentrating solar collectors and its applications *Appl. Energy* **101** 686–98

[7] Chaanaoui M, Vaudreuil S and Bounahmidi T 2016 Benchmark of Concentrating Solar Power Plants: Historical, Current and Future Technical and Economic Development *Procedia Comput. Sci.* **83** 782–9

[8] Chen F, Li M, Hassanien Emam Hassanien R, Luo X, Hong Y, Feng Z, Ji M and Zhang P 2015 Study on the optical properties of triangular cavity absorber for parabolic trough solar concentrator *Int. J. Photoenergy* **2015**

[9] Moya E Z 2012 7 - Parabolic-trough concentrating solar power (CSP) systems *Concentrating Solar Power Technology* Woodhead Publishing Series in Energy ed K Lovegrove and W Stein (Woodhead Publishing) pp 197–239

[10] Forristall R 2003 *Heat transfer analysis and modeling of a parabolic trough solar receiver implemented in engineering equation solver* (National Renewable Energy Lab., Golden, CO.(US))

[11] Mohamad K and Ferrer P 2019 Parabolic trough efficiency gain through use of a cavity absorber with a hot mirror *Appl. Energy* **238** 1250–7

[12] Fuqiang W and Ziming C 2017 Progress in concentrated solar power technology with parabolic trough collector system: A comprehensive review *Renew. Sustain. Energy Rev.* **79** 1314–28

[13] Ramchandra G. P, Sudhir V. P, Jyeshtharaj B. J and Vishwanath H. D Alternative designs of evacuated receiver for parabolic trough collector *Energy* **155** 66–76

[14] Wang P, Liu D Y and Xu C 2013 Numerical study of heat transfer enhancement in the receiver tube of direct steam generation with parabolic trough by inserting metal foams *Appl. Energy* **102** 449–60

[15] Sargent and Lundy LLC Consulting Group 2003 *Assessment of Parabolic Trough and Power Tower Solar Technology Cost and Performance Forecasts* (Chicago, Illinois: DIANE Publishing)

[16] International Renewable Energy Agency. Renewable energy technologies: cost analysis series: concentrating solar power; 2012.

[17] Antonaia A, Castaldo A, Addonizio M L and Esposito S 2010 Stability of W-Al 2 O 3 cermet based solar coating for receiver tube operating at high temperature *Sol. Energy Mater. Sol. Cells* **94** 1604–11

[18] Dudley V E, Kolb G J, Mahoney A R, Mancini T R, Matthews C W, Sloan M and Kearney D 1994 Test results: SEGS LS-2 solar collector *Nasa Stirecon Tech. Rep. N* **96**

[19] Forristall R 2004 EES heat transfer model for solar receiver performance *Proc. ISEC Sol.* 11–4

[20] Kennedy C E 2002 *Review of mid-to high-temperature solar selective absorber materials* (National Renewable Energy Lab., Golden, CO.(US))

[21] Kennedy C E and Price H 2005 Progress in Development of High-Temperature Solar-Selective Coating *ASME Int. Sol. Energy Conf. Sol. Energy* 749–55

[22] ASE Archimede Solar Energy

[23] Granqvist C G 1985 Spectrally Selective Coatings for Energy Efficiency and Solar Applications *Phys. Scr.* **32** 401

[24] Canan K 2013 Performance analysis of a novel concentrating photovoltaic combined system *Energy Convers. Manag.* **67** 186–96

[25] Miller D C, Khonkar H I, Herrero R, Antón I, Johnson D K, Hornung T, Schmid-Schirling T, Vinzant T B, Deutch S, To B, Sala G and Kurtz S R 2017 An end of service life assessment of PMMA lenses from veteran concentrator photovoltaic systems *Sol. Energy Mater. Sol. Cells* **167** 7–21

[26] Lampert C M 1979 Coatings for enhanced photothermal energy collection II. Non-selective and energy control films *Sol. Energy Mater.* **2** 1–17

[27] Grena R 2011 Efficiency Gain of a Solar Trough Collector Due to an IR-Reflective Film on the Non-Irradiated Part of the Receiver *Int. J. Green Energy* **8** 715–33

[28] Granqvist C G 1981 Radiative heating and cooling with spectrally selective surfaces *Appl. Opt.* **20** 2606–15

[29] Cyulinyana M C and Ferrer P 2011 Heat efficiency of a solar trough receiver with a hot mirror compared to a selective coating *South Afr. J. Sci.* **107** 01–7

[30] Kaluba V S, Mohamad K and Ferrer P 2020 Experimental and simulated performance of hot mirror coatings in a parabolic trough receiver *Appl. Energy* **257** 114020

[31] Kaluba V S and Ferrer P 2016 A model for hot mirror coating on solar parabolic trough receivers *J. Renew. Sustain. Energy* **8** 053703

[32] Mohamad K and Ferrer P Computational comparison of a novel cavity absorber for parabolic trough solar concentrators *Proc. 62th Annu. Conf. South Afr. Inst. Phys. SAIP2017 ArXiv190713066 Physicsapp-Ph*

[33] Mohamad K and Ferrer P Experimental and numerical measurement of the thermal performance for parabolic trough solar concentrators *Proc. 63th Annu. Conf. South Afr. Inst. Phys. SAIP2018 ArXiv190800515 Physicsapp-Ph*

[34] Mohamad K S B *Efficiency gain of the solar trough receiver using different optically active layers* Thesis (Johanesburg, South Africa: University of the Witwatersrand)

[35] Gnielinski V 1975 New equations for heat and mass transfer in the turbulent flow in pipes and channels *NASA STIrecon Tech. Rep. A* **75** 8–16

[36] Pech A J and Soberanis M E 2012 Efficiency curves analysis of a parabolic trough solar collector in the Yucatan Peninsula *J. Renew. Sustain. Energy* **4** 021203

[37] Mohamad K and Ferrer P 2021 Thermal performance and design parameters investigation of a novel cavity receiver unit for parabolic trough concentrator *Renew. Energy* **168** 692–704

[38] Jeter S M 1986 Calculation of the concentrated flux density distribution in parabolic trough collectors by a semifinite formulation *Sol. Energy* **37** 335–45

[39] Dudley V E, Kolb G J, Mahoney A R, Mancini T R, Matthews C W, Sloan M and Kearney D 1994 *Test Results: Segs Ls-2 Solar Collector* (Sandia National Labs., Albuquerque, NM (United States))

[40] Engineering ToolBox Thermal Conductivity of Metals, Metallic Elements and Alloys

[41] Mohamad K and Ferrer P 2019 Cavity receiver designs for parabolic trough collector *ArXiv190911053 Phys.*